Biochimica et Biophysica Acta 1853 (2015) 3083–3094

Contents lists available at ScienceDirect

Biochimica et Biophysica Acta

journal homepage: www.elsevier.com/locate/bbamcr

Review

Active cell mechanics: Measurement and theory☆

Wylie W. Ahmed [a,b,c,*], Étienne Fodor [d], Timo Betz [a,b,c]

[a] Institut Curie, Centre de recherche, 11, rue Pierre et Marie Curie, 75005 Paris, France
[b] Sorbonne Universités, Université Pierre et Marie Curie, Paris, France
[c] Centre National de la Recherche Scientifique, UMR168, Paris, France
[d] Laboratoire Matière et Systèmes Complexes, UMR7057, Université Paris Diderot, 75013 Paris, France

ARTICLE INFO

Article history:
Received 2 March 2015
Received in revised form 16 May 2015
Accepted 21 May 2015
Available online 27 May 2015

Keywords:
Cell mechanics
Nonequilibrium biophysics
Force measurement
Generalized Langevin Equation

ABSTRACT

Living cells are active mechanical systems that are able to generate forces. Their structure and shape are primarily determined by biopolymer filaments and molecular motors that form the cytoskeleton. Active force generation requires constant consumption of energy to maintain the nonequilibrium activity to drive organization and transport processes necessary for their function. To understand this activity it is necessary to develop new approaches to probe the underlying physical processes. Active cell mechanics incorporates active molecular-scale force generation into the traditional framework of mechanics of materials. This review highlights recent experimental and theoretical developments towards understanding active cell mechanics. We focus primarily on intracellular mechanical measurements and theoretical advances utilizing the Langevin framework. These developing approaches allow a quantitative understanding of nonequilibrium mechanical activity in living cells. This article is part of a Special Issue entitled: Mechanobiology.

1. Introduction

Living cells are complex machines that constantly consume energy to maintain their spatial and temporal organization [1,2]. This energy consumption is required to overcome the tendency to maximize entropic disorder, and is used to self-organize the cell. From the statistical mechanics point of view, a cell represents a system far away from thermodynamic equilibrium. This non-equilibrium behavior allows the organization and operation of complex mechanical processes at the molecular scale. The current interest in building nanoscale machines can greatly profit from such strategies as typical engineering methods break down at the small scale where thermal fluctuations dominate over directed and controlled movement. Furthermore, the study of working principles used by living cells provides interesting insight on how active mechanical forces can modify or even control the mechanical properties of a polymer network [3–5]. An interesting example is provided by strain stiffening [5], where the active contraction of molecular motors can increase the mechanical stiffness of a material by more than an order of magnitude.

The effect of active forces on self organization and material properties is a highly active research field [6–10]. Typical experimental approaches combine active mechanical measurements, with detailed analysis of the intracellular movement [4,11,131,132,134]. Furthermore, in recent years active gel theories have been successfully applied to describe and quantify flows and deformation within cells [10,12,13–16]. These active gel models have been recently reviewed [9,17]. Here we focus on experimental and theoretical approaches that allow local measurement and modeling of active systems. We define the term 'active mechanics' that integrates active components in the mechanical description of a material. A main part of this article describes Langevin-equation based approaches to derive the experimentally accessible quantities such as effective energy and force spectra using molecular properties of the underlying processes. This approach separates the contributions from thermal fluctuations and active forces to provide a framework to interpret and analyze activity measurements. Additionally, this approach does not rely on a hydrodynamic analysis as typically done in active gel theories. These active gel theories are optimal to describe active behavior on long timescales, where most biological material is considered fluid. In contrast, both the experimental and theoretical aspects of this work focus on a description of processes at intermediate and short timescales, where the viscoelastic material properties are dominant.

2. Experimental approaches

2.1. Principle of measurement

Advanced methods are used in materials science to determine the mechanical properties of a material, well known under the keyword

☆ This article is part of a Special Issue entitled: Mechanobiology.

* Corresponding author at: Institut Curie, Centre de recherche, 11, rue Pierre et Marie Curie, 75005 Paris, France.
E-mail address: wylie.ahmed@gmail.com (W.W. Ahmed).

http://dx.doi.org/10.1016/j.bbamcr.2015.05.022

rheology [18,19]. Rheology exploits the constitutive relation between stress (force per unit area) and strain (relative deformation) which is commonly known as Hooke's law, illustrated in Fig. 1a. The simplest form of this law ($F = kx$) describes how a force F, applied to an object with elastic constant k leads to a deformation x. This simplified law applies for 1D objects such as springs or rubber bands. To capture the geometric parameters of a 3D object the general form of Hooke's law $\sigma = E \times u$ is commonly used. Here the stress $\sigma = F/A$ is defined as the force F acting on a unit area A of the material. The strain $u = x/x_0$ corresponds to the relative deformation (Fig. 1a). Since the force direction with respect to the surface can be decomposed into normal or parallel components, the resulting deformation is found to be a tensile or shear deformation respectively. Depending on the type of deformation the mechanical properties are described by the Young's modulus E (normal deformation), the shear modulus G (shear deformation), or the bulk modulus K (uniform compression), as illustrated in Fig. 1a. In the case of linear elasticity, these different moduli are simple scalar numbers, related to each other by the Poisson's ratio v, that quantifies compressibility [20]. As we describe later, these moduli can become time, or frequency dependent to describe biological materials that are typically viscoelastic. In the more complex case of anisotropic materials, the introduced constitutive equation requires tensors, where the mechanical modulus becomes a fourth order tensor. In the following we only consider the case of isotropic material for simplicity, however, the described reasoning can be directly extended to a tensor notation.

In the context of living cells, the actual mechanical properties depend on the timescale of force application, and hence are described within the framework of viscoelastic materials. Here, the mechanical properties are decomposed into an elastic and a dissipative (viscous) component, where both may depend on the timescale investigated. The extreme case of pure elastic or purely viscous material is illustrated in Fig. 1b. The viscoelastic moduli are not scalars as in the pure elastic case, but functions of time or frequency. There are two main experimental strategies to determine the viscoelastic properties, namely the application of a step stress/strain, and the application of periodic stress/strain. A typical example of the first strategy is a creep experiment, where a step stress is applied resulting in a deformation of the material over time. Similarly, stress relaxation experiments can be used to apply a step deformation while measuring the stress in the system. The corresponding constitutive equation is $\sigma(t) = \int_{-\infty}^{t} E(t-t') \times \frac{du}{dt}|_{t'} dt'$. Here, the time dependent viscoelastic modulus $E(t)$ is replacing the scalar Young's modulus. If a step deformation is applied, the strain rate becomes a delta function that annihilates the integral, thus directly giving the viscoelastic properties as illustrated in Fig. 1c. While giving direct access to all timescales in one single experiment, practically this approach suffers from a low signal to noise ratio.

Modern rheometers avoid this problem by applying an oscillating stress and measuring the resulting time dependent strain. This results in a complex elastic modulus $G^*(\omega) = G'(\omega) + iG''(\omega)$ where the real part $G'(\omega)$ corresponds to the elastic energy stored in the material at timescales corresponding to the frequency ω (hence storage modulus) and the imaginary part $G''(\omega)$ corresponds to the energy dissipated by the viscous deformation (hence loss modulus) [18].

For measurement on the micron-scale, as relevant for living cells, typically a known force $F(t)$ is applied and the resulting absolute deformation $x(t)$ is monitored as a function of time [21–23]. Such experimental approaches, called active micro-rheology (AMR), give direct access to the mechanical response function χ that links an applied time dependent force to the resulting deformation via: $x(t) = \int_{-\infty}^{t} \chi(t-t') \times F(t')\,dt'$. This is equivalent to a convolution of the force with the time dependent response function. In the frequency domain it can hence be expressed as a multiplication of the Fourier transforms: $\tilde{x}(\omega) = \tilde{\chi}(\omega) \times \tilde{F}(\omega)$, where the tilde denotes for the Fourier transform of the corresponding variable. The transition from the response function to the shear modulus is provided by the Generalized Stokes–Einstein relation [21]: $G^*(\omega) = 1/(6\pi R\tilde{\chi}(\omega))$, where R is the radius of the probe particle. This last step assumes a homogenous and isotropic environment, which was already used when omitting the tensor notation.

The AMR methods directly probe the mechanical properties of the material. In contrast, passive microrheology approaches use the thermally driven particle fluctuations to access the dissipative part of the response function using the fluctuation dissipation theorem (FDT) $\tilde{C}(\omega) = \frac{2k_BT}{\omega}\tilde{\chi}''(\omega)$. Here $\tilde{C}(\omega)$ is the power spectral density that is calculated based on the particle trajectories by taking the square of the absolute value of the Fourier transform. Implicitly, this method assumes that the particle movement is driven purely by thermal movement and that the system is in thermodynamic equilibrium [24,25]. This assumption is known to be wrong in active systems such as living cells that are constantly consuming energy and are therefore non-equilibrium systems. For this reason, passive microrheology should only be used with care in living cells. Typically, in the high frequency regions fluctuations do not exhibit violation of the FDT [4,11]. Experimentally, 100 ms has been shown to be a typical timescale at

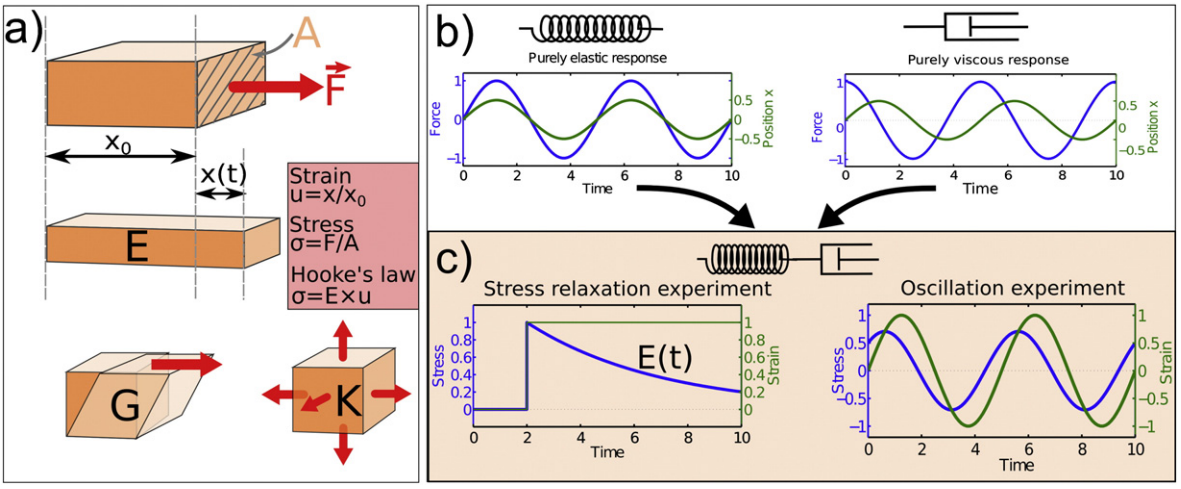

Fig. 1. Introduction of the mechanical principles to determine mechanics. (a) A force acting on a material applies a stress that will then create a strain. Depending on the deformation, the mechanical properties are described by a Young's modulus E, a shear modulus G or a bulk modulus K. (b) For viscoelastic materials the response can be separated into a purely elastic deformation that is in phase with an applied sinusoidal force, or a purely viscous deformation that has a 90° phase shift with the applied force. (c) Both combined give the information necessary to describe a viscoelastic material. The time dependent elastic moduli can be measured using step stress or strain experiments, as well as oscillating force application that gives information about the mechanics at the frequency of the applied force.

which active contributions emerge, both in reconstituted [4] and living systems [11]. However, this characteristic timescale should indeed depend on the cycling time of the active mechanical process, and might also be a function of the mechanical properties of the cell. On the other hand testing the validity of the FDT by comparing the directly measured response from AMR with the expected response calculated from spontaneous fluctuations is an elegant and direct way to determine the regimes of active and passive movements. For the study of active cell mechanics, the ideal experimental access is by a simultaneous measurement of both, the material properties such as the response function and/or the shear modulus by stress–strain measurements as well as the free particle motion via particle tracking. In the following we will briefly review the main techniques used for both of these measurements, with a special focus on the experimental setups that allow easy access to both the material properties and the free fluctuations.

2.2. Active measurement of mechanical properties

The direct measurement of the mechanical material properties requires both, a well defined force application and a precise measurement of the resulting deformation. On the cell level, the most common techniques providing this information are optical tweezers, magnetic tweezers and atomic force microscopy. Each of these methods has their technical advantages and limitations.

2.2.1. Optical tweezers (OT)

Optical tweezers use the gradient forces that act on polarizable materials in the center of a highly focused laser beam [26] (Fig. 2a). Typically, a high numerical aperture objective is used for both imaging and focusing of the laser. To provide stable 3D trapping a high numerical aperture objective is necessary to create sufficient axial gradient forces, which is required to balance scattering forces that push the particle out of the trap in the axial direction. To create a sufficient gradient force, high numerical apertures are required, and hence typically either oil or water immersion objectives with numerical apertures (NA) >1 are used [27]. While oil immersion objectives can provide higher NAs, and hence better 3D trapping they suffer from spherical aberration effects when the tweezers are used more than 10 μm away from the glass surface. These effects can be compensated in some objectives. Water immersion objectives do not have this inherent problem as long as the buffer solution in the experiment has a refractive index close to water. Therefore water immersion objectives allow optical tweezing up to working distances of hundreds of μm; however, with a slightly reduced trap stiffness due to the lower NA. When the experiment is done in close proximity to the coverslip, oil immersion objectives offer more advantages, while experiments in bulk should be performed using water immersion objectives. An interesting alternative is a double OT, where two counter-propagating lasers are focused on the same spot in 3D [28]. In such setups, the scattering force compensates and a small numerical aperture is sufficient for stable trapping. In consequence, long working distances up to mm can be realized [29].

Optical tweezers must be calibrated to determine the trap stiffness to calculate the force acting on the trapped particle as a function of the distance from the trap center. Calibration methods use the power spectral density of free particle fluctuations via the fluctuation dissipation theorem [30,31], the drag force method using the known viscosity of the medium [32] or Boltzmann distribution approach where the variance of the average particle position is associated to the trap stiffness of the tweezers [33]. These methods have been reviewed elsewhere [34]. A further elegant method is to directly infer the force by measuring the asymmetry of the scattered photons to directly determine the force using the conservation of momentum. This method, however, requires that all photons are collected after interaction with the sample which is achieved using a condenser with a higher NA than the objective [35].

To perform mechanical measurements either the laser focus or the sample itself must be displaced. To move the laser, piezo controlled mirrors [36] or acousto optical deflectors (AOD) [37,38] are commonly used. The mirrors have the advantage that the transverse laser mode is not influenced and the laser focus is continuously moving. The disadvantage of current piezo mirrors is their limited speed with maximal movements in the order of 1 kHz, and a limited angular travel of 1–10 mrad. Acousto optical deflectors exploit photon–phonon scattering, where both the intensity and the deflection angle can be controlled by

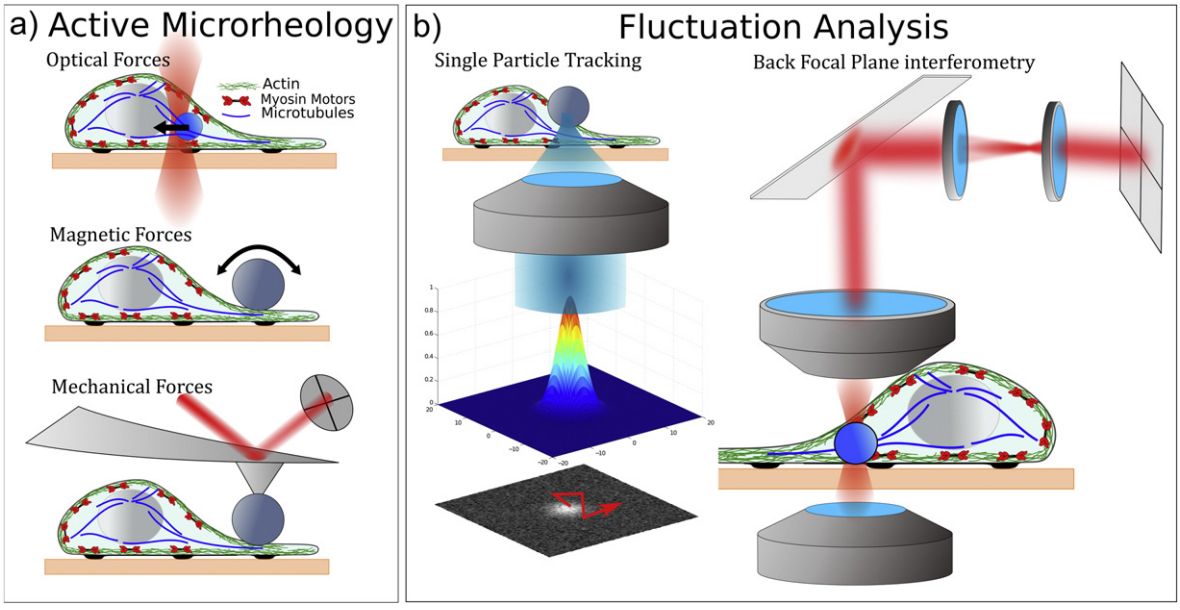

Fig. 2. Overview of the commonly used experimental methods to determine the local cell mechanics and the spontaneous particle movements. (a) Active microrheology methods provide detailed and local viscoelastic material properties. Commonly optical tweezers, magnetic tweezers, and optical magnetic twisting cytometry are used to assess intracellular and surface properties, while AFM typically measures the mechanics on the cell surface. (b) To determine the position of beads or organelles within cells, single particle methods image the fluorescence or bright field image, and then fit the expected intensity distribution to the image. This allows spatial precision down to several nm, with a time resolution depending on the image acquisition rate. Alternatively, back focal plane interferometry images the back focal plane of the condenser on a detector. After calibrating the detector response to the bead position, this can be used to gain sub-nm precision and high-speed (up to several hundred kHz) position information.

the intensity and frequency of a HF wave in a special birefringent crystal. AODs allow the trap to jump to arbitrary positions within a couple of μs, hence allowing for high speed measurements. The speed of the AODs is physically only limited by the time the acoustic wave needs to cross the laser beam size in the AOD. This high speed can be used to create multiple traps by rapid switching between multiple positions. If the switching frequency is an order of magnitude faster than the corner frequency of the power spectral density of the particle motion in the trap, it can be considered to be permanent for the particle despite the temporary absence. Downsides of the AODs are that during the switching, the laser focus is not well defined. Furthermore, if operating multiple tweezers via time-sharing, the actual calibration has to be done carefully in the same conditions as the final experiments are performed. Alternatively to switching, multiple traps can also be generated by superimposing several acoustic frequencies in the AOD. In optical tweezers, bead position is either detected using video microscopy or position sensitive detectors [39,40].

The response function can be measured by applying either an oscillating or a step force to intracellular particles such as endogenous vesicles or beads [11,41]. A step force protocol rapidly moves the laser or the stage and records the movement of the bead relaxing back into the laser focus. Step displacements probe the temporal dependence of the response function that can be translated to the frequency domain by a Fourier transform. In an oscillating force protocol, either the laser or the stage is moved with a sinusoidal function. The amplitude of this movement depends on the actual system, however, it has to be ensured that the applied movement is not exceeding the linear regime of the trap, which is determined by the bead size and the laser focus. To access different timescales, the same protocol is repeated for a series of frequencies. By observing the bead movement relative to the laser trap, both the applied forces, and the bead movement in the reference frame of the cell are determined. Dividing the Fourier transforms of the force and the displacement gives direct access to the real and imaginary part of the frequency dependent response function. The advantage of the oscillating force protocol is that by modulating a sine function with a well defined frequency, experimental and measurement noise can be filtered out by using lock-in amplifiers [4], or during post-processing of the data. The resulting response functions are very precise and the accuracy can be even increased by including more oscillations in the measurement. In contrast, the advantage of the step function is that the experiment does in parallel access all the different timescales, hence the experimental time is largely reduced, at the price of increased noise in the measurements.

2.2.2. Magnetic tweezers (MT) and optical magnetic twisting cytometry (OMTC)

An alternative method to apply well defined local forces is the magnetic tweezers [42,43]. Here either magnetic gradient forces create a well defined force on a paramagnetic particle [44], or oscillating magnetic fields create a torque on magnetic particles that are typically attached to the surface of a cell [43] (Fig. 2a). Magnetic tweezers and OMTC have the advantage of higher forces (up to 100 nN, [45]) and the absence of interaction between the magnetic field and the cell. The setup requires a strong magnetic gradient that can be generated by a variety of coil alignments [46]. Depending on the actual coil design, open cell culture dishes are often necessary to achieve high forces [45].

In the case of OMTC, ferromagnetic beads are incubated with the cells and attached to the surface either by specific receptors or by unspecific binding. A short, strong field (<1 s, >0.1 T) induces a horizontal magnetization in the beads. This is followed by a probe field that is applied vertically to the cells, hence applying a torque on the beads. This vertical field is typically weaker than the magnetization field (<0.01 T) and can be varied with a sinusoidal function, or a step force. With OMTC, high frequencies (>1 kHz) can be measured by controlling the applied oscillation frequency. The analysis of the frequency dependent measurements follows the same signal processing methods as described for the optical tweezers [47].

In both magnetic techniques, the bead movement is typically detected using video microscopy, where a precise trigger of the force application and the frame acquisition is important. Using single particle tracking algorithms, the position sensitivity of the bead motion measurement can be in the order of several nm. While the analysis of the response function and the shear modulus for magnetic tweezers is similar to optical tweezers, OMTC requires a model that connects the magnetic torque driven rotational movement to the elasticity of the underlying substrate. In this model the actual attachment area is an important parameter that is either taken from literature or is assessed via finite element modeling [48]. Errors in this factor will influence the absolute results, but not the relative comparisons.

Magnetic tweezers and OMTC have the advantage that they allow higher forces, and parallel application for forces on multiple particles, thus improving the possible applications and the throughput of the measurements.

2.2.3. Atomic force microscopy (AFM)

A third, commonly used method to locally measure the mechanical properties of living cells is atomic force microscopy. A flexible cantilever is used to indent the cell or object of interest [49–51]. The deflection of the cantilever is measured using a laser that is reflected off the surface of the cantilever tip and illuminates a quadrant photodiode as illustrated in Fig. 2a. To measure the mechanical properties of cells, the cantilever tip is typically spherical. This allows to use an analysis model such as the Hertz [52] or the Sneddon [53] model that describes the force as a function of indentation depth, using the mechanical properties of the substrate. These models are more complex compared to intracellular particles as the interaction area increases while the cantilever indents the cell. To asses the viscoelastic properties of the cells, a slow approach protocol can be added to a well defined oscillation. Using lock-in amplifiers this was demonstrated to access the localized frequency dependent viscoelastic properties of living cells [54,55]. Big advantages of the AFM are the large range of accessible forces, well developed commercial microscopes, and a large range of possible cantilever geometries. On the other hand, AFM measurements typically probe the cellular surface and not intracellular properties. It is possible to infer bulk properties with large indentation depths, however, interpretation is more difficult. Also, as cell chambers are open to allow cantilever access, special care for the correct conditions of the cells such as pH, temperature and osmolarity must be taken. Finally, AFMs do not allow parallel data acquisition. Still, AFMs are a main method to determine the mechanical properties of cells.

2.3. Measuring spontaneous fluctuations

In the absence of active mechanical forces, passive techniques have been used to successfully determine the mechanical properties of viscoelastic materials [21,56,57,133]. These techniques rely on precise measurement of the particle position, ideally in 3D. The trajectories of single particles are then used to either determine the mean square displacement (MSD), the autocorrelation, or the power spectral density, that are used to calculate the mechanical response function using equilibrium thermodynamic assumptions, such as the FDT. This method has been recently reviewed in detail [58].

In the presence of active forces, the measurement of spontaneous fluctuations provides information about both, the mechanical properties of the material but also the active forces that move the particle. In the absence of any additional access to the mechanical properties, however, it remains complicated to distinguish between the fluctuations that are due to the thermal agitation of the particle and the active forces [23]. This is especially true when the active forces act in an uncorrelated and isotropic way [59], hence showing statistical properties similar to thermal movement. The measurement of particle fluctuations is

typically done using either of the two main techniques: single particle tracking and laser interferometry (Fig. 2b).

2.3.1. Single particle tracking

Single particle tracking is a well established technique that has been introduced to determine diffusion coefficients from videomicroscopy [60–62]. This image based technique requires the acquisition of images either in bright field [63], or fluorescence microscopy, where the advantage of fluorescence microscopy is a high signal-to-noise ratio that allows for a better position measurement [64,65]. A downside of the fluorescence acquisition is that the sample often bleaches, thus limiting the total acquisition time. Bright field images are typically used if the particle to be tracked provides a strong contrast, such as optically trapped beads or magnetic beads, but can also be used on intracellular particles [63]. The tracking can be done by a number of open source programs, that vary in complexity, and which have been recently critically compared [39]. For the highest positional detection, modern algorithms fit the predicted function using the microscope specific point spread function to obtain subpixel resolution down to several nm. The big advantage of single particle tracking methods is the possibility to obtain simultaneously several particle traces. However, the particle tracking may require time intensive image processing and the temporal resolution depends on the image acquisition rate. This method is typically used in combination with magnetic tweezers, but also in many cases for optical tweezers [11,66].

2.3.2. Laser interferometry

An alternative tracking method uses a laser that is focused on the particle to be tracked [67–71]. After interacting with the particle, the scattered light and unscattered light create an interference pattern in the Fourier plane of the laser focus. This plane is imaged on either a position sensitive detector or a quadrant photodiode, that directly determines any asymmetry in the light illuminating the detector. These detectors then convert the photocurrent to a voltage that is measured using modern data acquisition boards. This voltage measures the illumination asymmetry in Δx and Δy, as well as the sum signal that corresponds to the total amount of light detected. After recording a calibration curve that maps the voltage difference to the distance of the particle from the laser focus, the movement of the particle can be followed with very high spatial ($<nm$) and temporal ($<10\ \mu s$) resolutions [37]. This technique is directly compatible with an optical tweezers setup, where the laser power is simply reduced to the μW range to prevent an influence of the particle due to optical trapping effects [72]. Using the sum signal or an additional detector, 3D tracking is also possible [73]. However, in case the particle moves out of the linear regime of the calibration curve the laser or the particle needs to be recentered in the laser focus. This limits the method to shorter tracks, typically of length smaller 400 nm, unless an automated repositioning is used. The advantage of this method is that it gives directly the 3D coordinates of the tracked particle with high spatial–temporal resolution while avoiding complex post-processing or data analysis. The laser tracking method is commonly used in optical tweezers as the setup requires only the addition of a position detector in the Fourier plane of the laser focus. Recently, laser tracking has even been used to track the complex shape fluctuations of helical bacteria [74].

2.4. Quantifying active mechanics

To get direct experimental access to the active contribution in the movement of an intracellular particle, detailed knowledge about the local mechanical properties is indispensable. Hence, the currently used methods to quantify the active mechanics in living cells measure both, the viscoelastic properties as well as the spontaneous fluctuations. It is important that these measurements are done on the same probe particle and without large time delay, as cellular systems vary both in time and space. In principle, the mechanics measurement itself might change the mechanical properties as it may trigger mechanosensing pathways that result in a restructuring of the cytoskeleton or an activation of motor proteins [75–77].

3. Theoretical models

3.1. Purpose and types of models

To get a deeper understanding of this nonequilibrium activity it is necessary to develop models to interpret the experimental measurements. For active cell mechanics, we focus on models that seek to understand what is happening at the level of the cytoskeleton and molecular motors. Hydrodynamic theories have made significant progress towards our understanding of active matter systems. These theories are based mainly on symmetries and do not involve specific microscopic details, and thus are applicable to a wide range of systems over varying scales. For extensive reviews of these approaches see [9,13,17,78]. These frameworks build on traditional hydrodynamics [79] by adding nonequilibrium forces and are primarily used for systems that are viscous at long time-scales. Recent theoretical advancements of active matter built upon previous theories have been applied to systems ranging from bacterial swarms [80,81] to large groups of organisms [82–85]. In this review, we focus on the Langevin framework for models of active mechanics which describes the motion of particles via a stochastic differential equation. We use this approach because it provides intuitive access to the model components. The Langevin approach introduces the activity via the active nonthermal noise which requires a microscopic description of the active process. Thus this approach is not generic like the hydrodynamic approach, but it offers straightforward coupling to molecular models. The purpose of this section is to do a simple walkthrough of the Langevin framework to provide a basis for readers unfamiliar with this topic to understand and develop their own simple models.

3.2. Langevin approach

The Langevin approach is the application of Newton's second law to a Brownian particle. It was the first example of a stochastic differential equation leading to the development of new fields in mathematics and physics [86]. Let's begin by describing Brownian motion in a purely viscous liquid using the Langevin framework. If we apply Newton's law ($F = ma$) to a Brownian particle we have the following equation of motion,

$$m\ddot{x} = -\gamma\,\dot{x} + \xi(t) \tag{1}$$

where m is the mass of the particle, $x(t)$ is its position and $\dot{x}, \ddot{x}$ represents the first and second time derivatives respectively, γ is the constant coefficient of friction, and $\xi(t)$ is the stochastic force that comes from thermal motion. In biological systems at the cell and molecular level the inertia is typically negligible (we can ignore the mass of the particle) and we have the overdamped form of the Langevin equation,

$$\gamma\,\dot{x} = \xi(t) \tag{2}$$

If we solve this equation for the particle trajectory,

$$x(t) = \frac{1}{\gamma}\int_0^t \xi(t')\mathrm{d}t' + x_0 \tag{3}$$

we see that the position of the particle, $x(t)$, depends on the entire history of the stochastic force, $\xi(t)$. This means that each time you solve Eq. (3) for the position of the particle it will be different depending on the specific realization of the stochastic force, $\xi(t)$, giving rise to the variation in trajectories of Brownian particles (Fig. 3a). For pure Brownian motion of a particle in a viscous liquid the stochastic force has the properties of

Gaussian white noise where the average force is zero, $\langle \xi(t) \rangle = 0$, and the forces are uncorrelated in time, $\langle \xi(t)\xi(t') \rangle = A\delta(t-t')$, where A is the amplitude of the thermal forces, and δ is the Dirac delta function. Now that we have the properties of the stochastic force, we can derive some properties of particle motion. First let's calculate the mean position of the particle over several realizations of the stochastic force,

$$\langle x(t) \rangle = \frac{1}{\gamma}\int_0^t \langle \xi(t') \rangle \mathrm{d}\, t' + x_0 \tag{4}$$

$$= x_0 \tag{5}$$

because $\langle \xi(t) \rangle = 0$. Thus, on average a particle stays at its original starting point when averaged over many realizations of the stochastic force (as expected). This is not very exciting. A more exciting metric is the mean squared displacement (MSD) of the particle which should resemble perfect diffusion in a purely viscous liquid. To calculate the MSD let us first take the square of the position in Eq. (3) to get,

$$x(t)^2 = \frac{1}{\gamma^2}\int_0^t\int_0^t \xi(t_1)\xi(t_2)\mathrm{d}\, t_1 \mathrm{d}\, t_2 + x_0^2 + \frac{2}{\gamma}x_0\int_0^t \xi(t')\mathrm{d}t' \tag{6}$$

and by taking the properties of the stochastic force we have,

$$\left\langle x(t)^2 \right\rangle - x_0^2 = \frac{1}{\gamma^2}\int_0^t A\,\mathrm{d}t_1 \tag{7}$$

$$= \frac{A}{\gamma^2}t \tag{8}$$

which is the familiar result that the MSD is proportional to time for a particle undergoing thermal diffusion in a purely viscous liquid. We can compare this to the original result derived by Einstein [87] that $\langle x(t)^2 \rangle = 2Dt$ where $D = \frac{k_B T}{\gamma}$ is the diffusion coefficient. This comparison also allows us to equate the amplitude of thermal force to the diffusion coefficient to find the fluctuation–dissipation theorem of the second kind,

$$A = 2\gamma k_B T \tag{9}$$

showing that the amplitude of the thermal forces is directly related to the friction coefficient and the temperature. This example shows how the Langevin framework can be used in a straight-forward fashion to describe stochastic motion in an intuitive way.

3.3. Models of mechanics

Once the equation of motion, $x(t)$, is known it is possible to derive the mechanical behavior of medium in thermal equilibrium in two steps. First we apply linear-response theory (LRT), $x(t) = \int_{-\infty}^{t}\chi(t-t')F(t')\,\mathrm{d}t'$, to calculate the response of the system $x(t)$ to a force, $F(t)$. Second, we apply the Generalized Stokes–Einstein (GSE) equation [88,89] to calculate the complex shear modulus which represents the mechanical behavior of the system.

Let's first describe the mechanics of the purely viscous liquid described in the previous section. Often times in mechanics it is more intuitive (and mathematically tractable) to work in the frequency domain. Eq. (2) written in the Fourier domain is,

$$i\omega\gamma\tilde{x} = \tilde{\xi} \tag{10}$$

Now if we apply linear response theory, $\tilde{x} = \tilde{\chi}\tilde{F}$, where we know that the force acting on the particle is the thermal force $\left(\tilde{F}_{\text{thermal}} = \tilde{\xi}\right)$ then we can deduce the response function,

$$\tilde{\chi} = \frac{1}{i\omega\gamma} \tag{11}$$

To get the complex shear modulus we use the GSE, $G^* = \frac{1}{6\pi R\tilde{\chi}}$, to find

$$G^*_{\text{liquid}} = \frac{i\omega\gamma}{6\pi R} \tag{12}$$

where R is the radius of the particle. Notice if we separate the complex modulus into its elastic (G') and viscous (G'') components then we have,

$$G'_{\text{liquid}} = 0 \tag{13}$$

$$G''_{\text{liquid}} = \frac{\omega\gamma}{6\pi R} \tag{14}$$

and we can see that a purely viscous liquid provides no elastic resistance and its viscous resistance scales linearly with frequency as shown by the open circles in Fig. 3b.

The complex shear modulus of a purely elastic solid can be derived similarly as above. If we represent the elasticity of the material using a simple harmonic potential ($E = \frac{1}{2}\kappa x^2$) then the equation of motion is,

$$\kappa\tilde{x} = \tilde{\xi} \tag{15}$$

where κ is the stiffness of the harmonic potential. Applying LRT and GSE we have,

$$G'_{\text{solid}} = \frac{\kappa}{6\pi R} \tag{16}$$

$$G''_{\text{solid}} = 0 \tag{17}$$

where for a simple harmonic spring the shear modulus is not dependent on frequency (see Fig. 3b, closed circles). This result is consistent with the sketched representation as shown in Fig. 1, where purely elastic response is fully in phase of an oscillating force, while a purely viscous response is out-of phase.

Since most biological materials are not purely viscous or purely elastic it is typically necessary to describe them as viscoelastic. Incorporating both of these effects leads to an equation of motion for a particle that contains both viscous and elastic terms,

$$i\omega\tilde{\gamma}\tilde{x} = -\kappa\tilde{x} + \tilde{\xi} \tag{18}$$

These terms $(\tilde{\gamma}, \kappa)$ can take on various forms to describe different viscoelastic systems. The cytoskeleton is often described as a semi-flexible polymer network which exhibits power-law rheology at high frequencies with a low frequency elastic plateau [90–92]. A simple way to describe this is to adopt a power-law memory kernel for $\gamma(t) = \frac{\kappa(\tau_\alpha/t)^\alpha}{\Gamma(1-\alpha)}$, where $0 < \alpha < 1$ is the power-law scaling, τ_α is the viscoelastic time constant, and Γ is the Gamma function. Taking the Fourier transform yields $\tilde{\gamma} = \kappa\tau_\alpha(i\omega\tau_\alpha)^{\alpha-1}$. Following the same procedure as before and applying LRT and GSE gives us,

$$G'_{\text{viscoelastic}} = \frac{1}{6\pi R}\left[\kappa\tau_\alpha^\alpha\omega^\alpha\cos(\pi\alpha/2) + \kappa\right] \tag{19}$$

$$G''_{\text{viscoelastic}} = \frac{1}{6\pi R}\left[\kappa\tau_\alpha^\alpha\omega^\alpha\sin(\pi\alpha/2)\right] \tag{20}$$

as shown in Fig. 3b (squares).

3.4. Models of activity

Now that we have derived the mechanical response of the system in the Langevin framework, we can turn to the purpose of this review which is adding nonequilibrium forces. In the previous section on mechanics, notice that the only stochastic force involved is thermal in nature because the systems are in thermal equilibrium. This is because

material properties are typically defined for materials in thermal equilibrium. For systems that are out-of-equilibrium, such as biological systems, there are additional forces coming from processes occurring inside the cell (e.g. molecular motors and polymerization). The advantage of the Langevin framework is that additional forces can be intuitively incorporated into the equation of motion of the particle [131]. As an example, let us add a stochastic force that is non-thermal in origin to the right side of the equation of motion for a viscoelastic material. Thus we have,

$$i\omega\tilde{\gamma}\tilde{x} = -\kappa\tilde{x} + \tilde{\xi} + \tilde{f}_A \tag{21}$$

where f_A is the stochastic active force. The active force can be modeled in many ways to account for different physical systems. Using this approach, a molecular scale model of the active force can be developed and incorporated into the Langevin framework. Additionally, if the form of the active force is too complex to be solved analytically, it can straightforwardly be explored via simulations. Thus predictions for the average dynamics of objects inside the cell can be calculated, allowing close comparison between experiments and theory. As an example, we will present a simple minimal model for the active force, f_A, that has been described previously [93,94] and is illustrated in Fig. 4a. This model describes the force contribution from molecular motors that actively kick the particle and cause it to move around randomly. The force due to this motion can be expressed as, $f_A = \kappa\int v_A(t')dt'$ where v_A is the active velocity described by a random process that equals 0 for an average duration of τ_0 and is a uniform random value over $[-v, v]$ for an average duration of τ. The statistics of v_A reflect molecular motor statistics and are a zero mean non-Gaussian process with correlations: $\langle v_A(t)v_A(t')\rangle = k_BT_A exp(-|t|/\tau)/(\tau\gamma)$ where $k_BT_A = \frac{\gamma(v\tau)^2}{3(\tau+\tau_0)}$ is the effective active energy scale [93,94]. A representative realization of the motor force kinetics is shown in Fig. 4b.

Now that we have the equation of motion for a particle in a viscoelastic material subjected to an active stochastic force we can explore some of the system properties. A common way to quantify the nonequilibrium properties of a system is to calculate its effective energy, which quantifies deviation from equilibrium. This requires combining information from the mechanical response, $\tilde{\chi}''(\omega)$, and the spontaneous fluctuations, $\tilde{C}(\omega)$, of the particle motion where $\tilde{C}(\omega) = \int\langle x(t)x(0)\rangle exp(i\omega t)dt$ is the power spectral density of position fluctuations. The effective energy is basically the ratio of these two, $E_{\text{eff}} = \frac{\omega\tilde{C}(\omega)}{2\tilde{\chi}''(\omega)}$, in units of k_BT. In the experimental measurements the response is calculated from active rheology and the spontaneous fluctuations are from particle tracking. For our example theoretical model this can be calculated as,

$$E_{\text{eff}}(\omega) = k_BT + \frac{1}{(\omega\tau_r)^2}\frac{k_BT_A}{1+(\omega\tau)^2} \tag{22}$$

where $\tau_r = \gamma/\kappa$ is the relaxation time of the surrounding material, and it is clear if T_A is zero the system is in thermal equilibrium (Fig. 4c). While the effective energy provides a way to quantify the deviation from equilibrium, it does not directly provide insight into the active forces generated in the system. To gain insight into the active mechanics we must look at the force correlations. First, let us note that the total force driving the system is the sum of the active force and thermal force, $\tilde{F}_{\text{tot}} = \tilde{f}_A + \tilde{\xi}$. Following the derivation above we can find that the mechanical properties of the system are, $G^* = \frac{1}{6\pi R}(\kappa + i\omega\gamma)$, where κ and γ are constants for simplicity that are related to the elastic and viscous properties of the system. This framework now allows direct access to the active force spectrum that is generated exclusively from nonequilibrium sources. To look at the active forces we calculate its power spectrum (i.e. the Fourier transform of the time correlation function $\langle f_A(0)f_A(t')\rangle$),

$$S_{\text{active}}(\omega) = \frac{1}{(\omega\tau_r)^2}\frac{2\gamma k_BT_A}{1+(\omega\tau)^2} \tag{23}$$

as is shown in Fig. 4d [93]. Thus it is clear that the mechanical properties of the surrounding material also contribute to the active forces. Again, notice that if the system is in equilibrium, $T_A = 0$, then the active force spectrum would be zero. The analytical expression of the active force spectrum can be fitted to the experimental measurements to extract the characteristic timescale, τ, of the molecular process driving the nonequilibrium behavior. This provides a connection between the observable motion of a tracer particle and the underlying stochastic driving forces.

Recent developments in stochastic thermodynamics leverage the Langevin framework to allow quantification of the rate of energy dissipation [95]. Energy dissipation is a fundamental property that characterizes non-equilibrium steady-state systems and allows comparison between different model systems. The Harada–Sasa equality relates the violation of the FDT to the amount of energy dissipated in the system. Therefore, if violation of FDT can be measured and modeled, the energy dissipation can be directly calculated and related to a

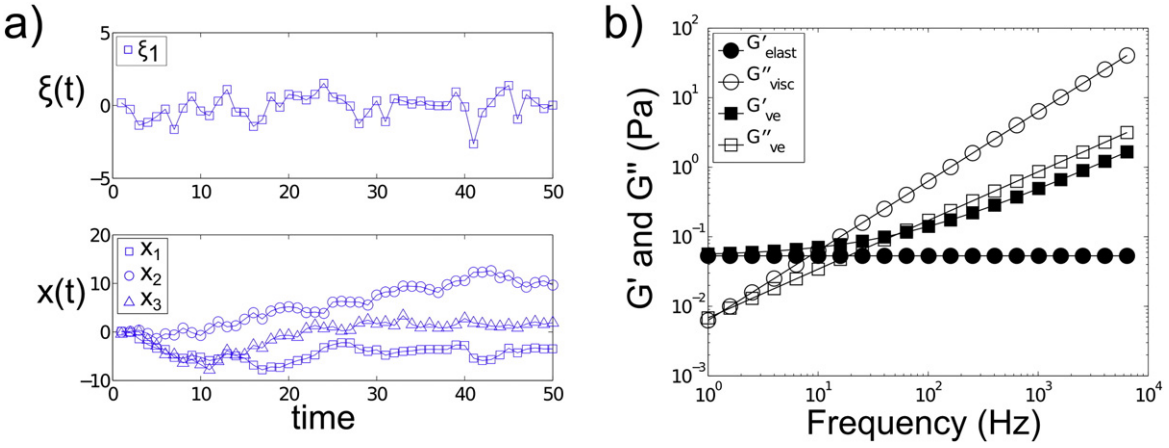

Fig. 3. (a) One realization of the stochastic thermal force is shown to illustrate the time course of a zero-mean Gaussian process (ξ_1, top panel). The trajectory of a particle, $x(t)$, is found by integrating the random thermal force, $\xi(t)$, over time as shown in 3 separate realizations (lower panel). (b) The complex shear modulus is shown for three different models of mechanics. A purely viscous liquid has dissipative modulus, G'', that scales linearly with frequency (open circles). A purely elastic solid has an elastic modulus, G', that is frequency independent (closed circles). A viscoelastic material exhibits intermediate behavior with frequency dependent elastic and dissipative moduli.

molecular scale model. In this framework the dissipation in the system is the work done by the particle on the surrounding environment. The mean rate of energy dissipation is,

$$J_{\text{diss}} = \langle \dot{x}\,(\gamma\,\dot{x} - \xi)\rangle \tag{24}$$

where $\dot{x}$ is the particle velocity. J_{diss} can be thought of as the difference between the power dissipated by the particle drag force ($\gamma\dot{x}$) and the power injected by the thermal force (ξ). In an equilibrium process, these two powers are equal as a consequence of FDT, and thus J_{diss} would be zero. Harada and Sasa showed that the dissipated power in a nonequilibrium steady state system can be calculated from the correlation and response functions [95],

$$J_{\text{diss}} = \gamma \int d\omega \left[\omega \tilde{C}(\omega) + 2T\tilde{\chi}''(\omega)\right]\omega/2\pi \tag{25}$$

where $\tilde{C}(\omega)$ is the power spectral density of the position fluctuations and $\tilde{\chi}''(\omega)$ is the imaginary part of the response function. Since all the terms in the Harada–Sasa relation can be measured experimentally and modeled theoretically, it provides a direct way to compare experimental and theoretical results of local power dissipation in nonequilibrium steady-state systems. Since power dissipation is a fundamental thermodynamic quantity it is possible to relate these measurements to the mechanical efficiency of a process.

4. Nonequilibrium biopolymer mechanics

The theoretical tools in the previous section provide a useful framework to understand the complex mechanics of nonequilibrium biopolymers and reconstituted in-vitro networks provide a simple experimental system to probe their behavior. It is known that external stress/strain applied to reconstituted biopolymer gels can lead to both softening and stiffening. Complex interactions at the local molecular scale can give rise to bulk changes in behavior even without active forces. Stress-softening has been attributed to local buckling of actin filaments [96], force induced rupture of cross-links [97], and nonlinear force response and filament turnover [98]. Stress stiffening has been shown to be due to network structure [99,100], dynamic rebinding of cross-links [101,102], and cyclic-loading [103].

4.1. Softening

An entangled polymer solution naturally exhibits viscoelastic mechanical behavior. If molecular motors are added to the entangled polymer, its properties can be actively modulated. Myosin-II motor activity in a solution of entangled actin filaments will significantly shorten the stress relaxation time leading to fluidization of the material [3] (Fig. 5a). Myosin-II motors interact with the actin and allow filaments to slide longitudinally past each other leading to bulk fluidization. A theoretical model shows that the active forces generate directed reptation of the polymers leading to fluidization [104]. Together, these studies indicate a way that internally generated active forces can tune the bulk mechanical properties of the material without physically changing its building blocks. A similar study showed that adding cross-linking can increase the energy dissipation in active actin networks at short timescales while still allowing fluidization at longer times [105]. This points to the high sensitivity of biopolymer network mechanics to motor activity and cross-linking which can provide a way to tune the material properties [106]. In addition to tuning material properties, myosin-II motors have been shown to buckle, fragment, and depolymerize actin filaments, directly changing the network and leading to stress relaxation [107–109]. These controlled in-vitro studies show possible mechanisms that living cells could utilize to tune their mechanical behavior. In living cells it has been reported that force application fluidizes the cell mechanical properties [110] as measured by magnetic twisting cytometry. Direct measurement in living cells is sparse, however some studies have shown that applied deformation may also lead to decreased cytoplasmic resistance [111,112]. And metabolic activity was shown to fluidize the cytoplasm and facilitate motion of larger components in bacteria cells [113]. Another recent study has used several different measurement techniques to show that myosin-II activity softens cells in suspension [114]. Further measurements and theories are necessary to understand these processes at the molecular level.

4.2. Stiffening

Stiffening due to motor activity is also a common observation. A landmark study of nonequilibrium mechanics in active actin–myosin gels showed that cross-linked networks stiffen (by up to 100×) due to the action of molecular motors [4] (Fig. 5b). A theoretical model showed that even small forces generated by molecular motors in a semi-flexible gel (exhibiting nonlinear elasticity) lead to a strong stiffening of the network [115,116]. It has been suggested that cells operate in this highly sensitive nonlinear regime such that small changes in motor activity allow them to modulate their mechanical response greatly [5]. Interestingly, a recent study created an active gel using noncytoskeletal components (DNA and FtsK50C) and found similar results, highlighting that the observed behavior is not specific to actin and myosin [118]. Similar behavior has been observed indirectly in living cells. Single platelet cells increase their bulk stiffness when allowed to contract between two rigid surfaces [119]. In living oocytes the stiffness of the cortex is maintained by myosin-II activity, and it dramatically softens if these motors are excluded [120]. And in the cytoplasm of cultured cells the stiffness has also been shown to decrease when myosin-II motors are deactivated via blebbistatin [11]. It is important to mention that the studies discussed here in living cells make direct force measurements, which allow direct access to the mechanical properties. Generally, it should be noted that studies in living cells must be interpreted carefully since their response to pharmacological treatment and genetic tools is often highly sensitive to dosage and recovery time.

4.3. Active organization

In addition to nonequilibrium mechanics, an interesting property of active matter is its ability to dynamically self-organize. High-density motility assays of actin filaments, myosin-II motors, and cross-linking proteins have shown a wide range of self-organization phenomena ranging from large-scale polar structures to contracting networks [121]. Collective motion emerges from the random molecular motor activity on polar actin filaments leading to coherent moving structures with clusters, swirls, and interconnected bands due to hydrodynamic coupling between filaments [122,123]. These complex interactions also give rise to frozen steady-states and giant fluctuations in density [124,125]. Beyond these dynamic moving structures, active actin-gel networks can also form quasi-static heterogeneous structures in the form of clusters of different sizes [126]. Interestingly, studies of active matter consisting of microtubules and kinesin also show active organization that is quite different from actin–myosin gels. Bundles of microtubules containing hundreds of kinesin motors spontaneously synchronize their motion and generate large-scale oscillations [127], suggesting that only two-components are sufficient to create cilia-like beating. When the microtubule–kinesin network is assembled inside an emulsion droplet, it exhibits internally driven chaotic flows leading to fractures and self-healing of microtubules and also drives autonomous motility of the droplet [128]. To mimic cellular structures the microtubule–kinesin network was encapsulated in a lipid vesicle where it exhibited periodically oscillating active nematic defects and shape-changing dynamics with filopodia-like

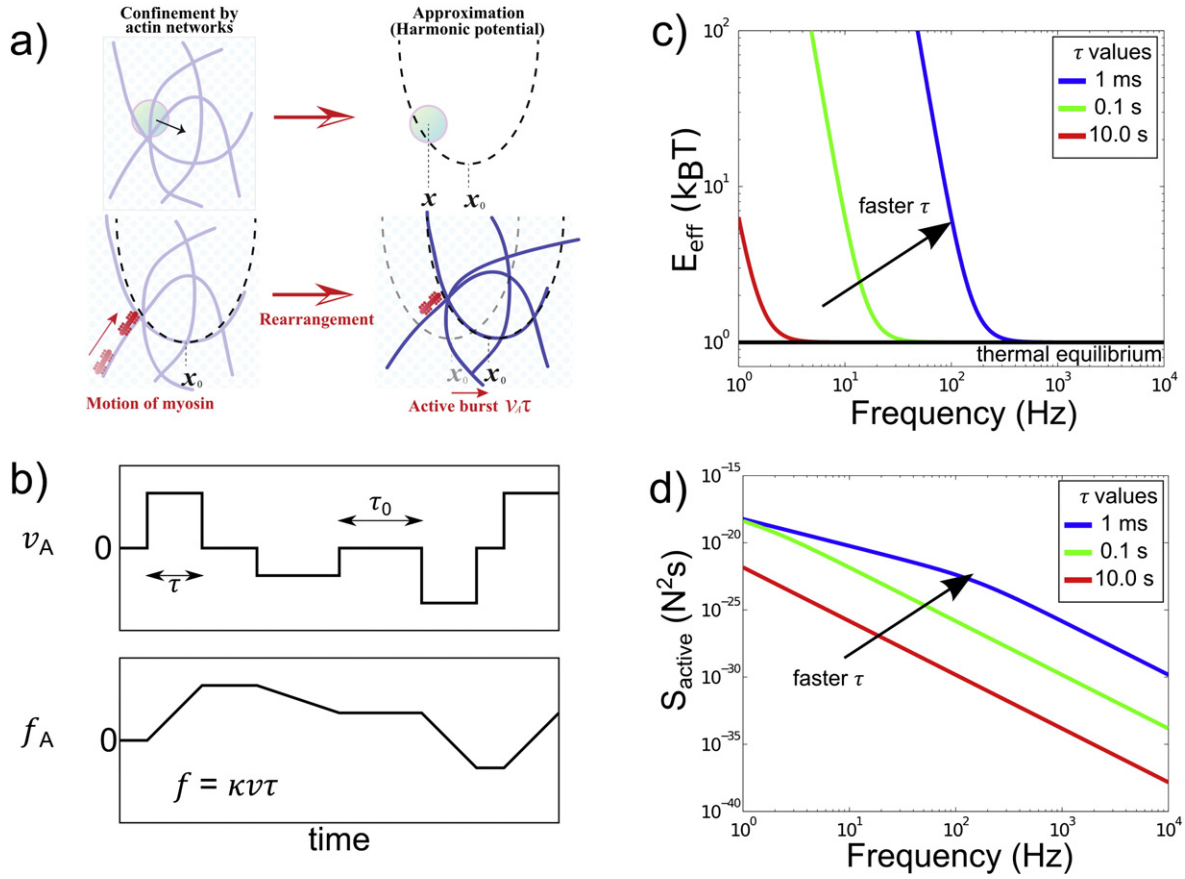

Fig. 4. (a) A schematic diagram of the viscoelastic material with motor-driven activity. The surrounding medium provides local confinement of particles modeled as a harmonic potential. Particles embedded in the material undergo thermal fluctuations with a mean position of x_0. In addition, molecular motors inject nonequilibrium activity into the system and push the particle further from the equilibrium position giving rise to additional forces that are nonthermal in origin. (b) Molecular motor statistics are modeled as an active burst where they have a velocity v_A, which is a random value between $-v$ and v for a random duration of order τ followed by a velocity of 0 for average duration τ_0 (top panel). The example realization of active burst activity results in the active forces shown in the lower panel. (c) The effective energy quantifies how far the system is from equilibrium. The activity is determined by the motor kinetics, where faster τ results in deviation from equilibrium at higher frequencies. (d) The active force spectrum quantifies the forces generated by the motor-driven activity. In the presented model faster motor kinetics, τ, result in higher active forces.
(b) Reprinted with permission from [94] Copyright (2014) by the American Physical Society.

protrusions [129]. These reconstituted active matter systems bring us closer to understanding how cells utilize activity to organize their functional structures. A recent example was observed in living oocytes where coordinated molecular motor activity generates a gradient force to center the nucleus at the cell center [130].

5. Outlook

Nonequilibrium activity is required for the maintenance of life. Without it, all systems decay to their lowest energy state corresponding to maximum disorder. For living cells to maintain their

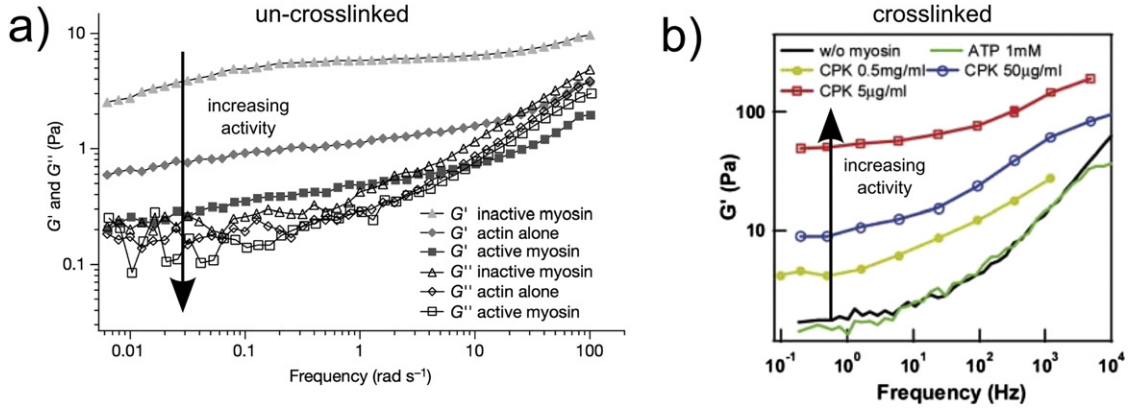

Fig. 5. (a) Un-crosslinked actin–myosin networks exhibit significantly smaller shear moduli when myosin is active. This is an example of activity-induced softening of an active material. (b) Conversely, cross-linked actin–myosin networks exhibit significantly larger shear moduli when myosin is active, an example of activity-induced stiffening.
(a) Adapted by permission from Macmillan Publishers Ltd: [3], Copyright (2002). (b) From reference [4]. Reprinted with permission from AAAS.

cytoskeletal structure, organization, and dynamic behavior they must constantly consume and dissipate energy. By understanding how this nonequilibrium activity drives self-organization we will gain a deeper understanding of biophysical processes at the molecular scale. The emerging experimental and theoretical frameworks to probe nonequilibrium mechanics will allow direct quantification of activity in living cells and allow us to dissect the complex underlying processes. These same techniques can also be applied to synthetic or reconstituted systems to understand fundamental processes in nonequilibrium physics. This interface between living cells and synthetic systems will undoubtedly lead to the design and engineering of new bio-inspired materials with advanced functionalities.

Acknowledgements

We thank Paolo Visco and Frédéric van Wijland for their helpful discussions. WWA is a recipient of post-doctoral fellowships from La Fondation Pierre-Gilles de Gennes and Marie Curie Actions. TB was supported by the French Agence Nationale de la Recherche (ANR) grant ANR-11-JSV5-0002 and LabEx CelTisPhyBio grant No. ANR-10-LBX-0038.

References

[1] A.S. Mikhailov, B. Hess, Self-Organization in Living Cells: Networks of Protein Machines and Nonequilibrium Soft Matter, J. Biol. Phys. 28 (4) (December 2002) 655–672.
[2] F.C. Mackintosh, C.F. Schmidt, Active cellular materials, Curr. Opin. Cell Biol. 22 (1) (February 2010) 29–35.
[3] D. Humphrey, C. Duggan, D. Saha, D. Smith, J. Kas, Active fluidization of polymer networks through molecular motors, Nature 416 (6879) (March 2002) 413–416.
[4] D. Mizuno, C. Tardin, C.F. Schmidt, F.C. MacKintosh, Nonequilibrium mechanics of active cytoskeletal networks, Science 315 (5810) (January 2007) 370–373.
[5] G.H. Koenderink, Z. Dogic, F. Nakamura, P.M. Bendix, F.C. MacKintosh, J.H. Hartwig, T.P. Stossel, D.A. Weitz, An active biopolymer network controlled by molecular motors, Proc. Natl. Acad. Sci. 106 (36) (September 2009) 15192–15197.
[6] S. Wang, P.G. Wolynes, Active contractility in actomyosin networks, Proc. Natl. Acad. Sci. U. S. A. 109 (17) (April 2012) 6446–6451.
[7] R. Levayer, T. Lecuit, Biomechanical regulation of contractility: spatial control and dynamics, Trends Cell Biol. 22 (2) (February 2012) 61–81.
[8] M. Soares e Silva, M. Depken, B. Stuhrmann, M. Korsten, F.C. MacKintosh, G.H. Koenderink, Active multistage coarsening of actin networks driven by myosin motors, Proc. Natl. Acad. Sci. 108 (23) (June 2011) 9408–9413.
[9] J. Prost, F. Jülicher, J.-F. Joanny, Active gel physics, Nat. Phys. 11 (2) (February 2015) 111–117.
[10] K. Kruse, J.F. Joanny, F. Jülicher, J. Prost, K. Sekimoto, Asters, Vortices, and Rotating Spirals in Active Gels of Polar Filaments, Phys. Rev. Lett. 92 (7) (February 2004) 078101.
[11] M. Guo, A.J. Ehrlicher, M.H. Jensen, M. Renz, J.R. Moore, R.D. Goldman, J. Lippincott-Schwartz, F.C. MacKintosh, D.A. Weitz, Probing the stochastic, motor-driven properties of the cytoplasm using force spectrum microscopy, Cell Camb. MA 158 (4) (August 2014) 822–832.
[12] H. Turlier, B. Audoly, J. Prost, J.F. Joanny, Furrow constriction in animal cell cytokinesis, Biophys. J. 106 (1) (January 2014) 114–123.
[13] J.F. Joanny, J. Prost, Active gels as a description of the actin myosin cytoskeleton, HFSP J. 3 (2) (2009) 94–104.
[14] K. Kruse, J.F. Joanny, F. Jülicher, J. Prost, K. Sekimoto, Generic theory of active polar gels: a paradigm for cytoskeletal dynamics, Eur. Phys. J. E 16 (1) (January 2005) 5–16.
[15] S. Ramaswamy, M. Rao, Active-filament hydrodynamics: instabilities, boundary conditions and rheology, New J. Phys. 9 (11) (November 2007) 423.
[16] A.J. Levine, F.C. MacKintosh, The Mechanics and Fluctuation Spectrum of Active Gels, J. Phys. Chem. B 113 (12) (March 2009) 3820–3830.
[17] M.C. Marchetti, J.F. Joanny, S. Ramaswamy, T.B. Liverpool, J. Prost, M. Rao, R. Aditi Simha, Hydrodynamics of soft active matter, Rev. Mod. Phys. 85 (3) (July 2013) 1143–1189.
[18] R.S. Lakes, Viscoelastic Solids, CRC Press, October 1998.
[19] F.A. Morrison, Understanding Rheology, Oxford University Press, New York, January 2001.
[20] G.N. Greaves, A.L. Greer, R.S. Lakes, T. Rouxel, Poisson's ratio and modern materials, Nat. Mater. 10 (11) (November 2011) 823–837.
[21] A.J. Levine, T.C. Lubensky, One- and Two-Particle Microrheology, Phys. Rev. Lett. 85 (8) (August 2000) 1774–1777.
[22] A.R. Bausch, F. Ziemann, A.A. Boulbitch, K. Jacobson, E. Sackmann, Local measurements of viscoelastic parameters of adherent cell surfaces by magnetic bead microrheometry, Biophys. J. 75 (4) (October 1998) 2038–2049.
[23] D. Mizuno, D.A. Head, F.C. MacKintosh, C.F. Schmidt, Active and Passive Microrheology in Equilibrium and Nonequilibrium Systems, Macromolecules 41 (19) (October 2008) 7194–7202.
[24] H.B. Callen, T.A. Welton, Irreversibility and Generalized Noise, Phys. Rev. 83 (1) (July 1951) 34–40.
[25] R. Kubo, The fluctuation-dissipation theorem, Rep. Prog. Phys. 29 (1) (January 1966) 255.
[26] A. Ashkin, J.M. Dziedzic, J.E. Bjorkholm, S. Chu, Observation of a single-beam gradient force optical trap for dielectric particles, Opt. Lett. 11 (5) (May 1986) 288–290.
[27] S. Nader, S. Reihani, L.B. Oddershede, Improving optical trapping in the axial direction and a continuous change of the optimal trapping depth, Proc. SPIE 6644, Optical Trapping and Optical Micromanipulation IV 2007, p. 664421.
[28] S.B. Smith, Y. Cui, C. Bustamante, Optical-trap force transducer that operates by direct measurement of light momentum, Methods Enzymol. 361 (2003) 134–162.
[29] Z. Bryant, M.D. Stone, J. Gore, S.B. Smith, N.R. Cozzarelli, C. Bustamante, Structural transitions and elasticity from torque measurements on DNA, Nature 424 (6946) (July 2003) 338–341.
[30] K. Berg-Sørensen, H. Flyvbjerg, Power spectrum analysis for optical tweezers, Rev. Sci. Instrum. 75 (3) (March 2004) 594–612.
[31] P.M. Hansen, I. Marija Tolic-Nørrelykke, H. Flyvbjerg, K. Berg-Sørensen, tweezercalib 2.1: Faster version of MatLab package for precise calibration of optical tweezers, Comput. Phys. Commun. 175 (8) (October 2006) 572–573.
[32] R.M. Simmons, J.T. Finer, S. Chu, J.A. Spudich, Quantitative measurements of force and displacement using an optical trap, Biophys. J. 70 (4) (April 1996) 1813–1822.
[33] E.-L. Florin, A. Pralle, E.H.K. Stelzer, J.K.H. Horber, Photonic force microscope calibration by thermal noise analysis, Appl. Phys. A Mater. Sci. Process. 66 (7) (1998) S75–S78.
[34] K.C. Neuman, S.M. Block, Optical trapping, Rev. Sci. Instrum. 75 (9) (2004) 2787–2809.
[35] A. Farré, M. Montes-Usategui, A force detection technique for single-beam optical traps based on direct measurement of light momentum changes, Opt. Express 18 (11) (May 2010) 11955–11968.
[36] M. Mahamdeh, E. Schäffer, Optical tweezers with millikelvin precision of temperature-controlled objectives and base-pair resolution, Opt. Express 17 (19) (September 2009) 17190–17199.
[37] M. Bussonnier, K. Carvalho, J. Lemière, J.-F. Joanny, C. Sykes, T. Betz, Mechanical Detection of a Long-Range Actin Network Emanating from a Biomimetic Cortex, Biophys. J. 107 (4) (August 2014) 854–862.
[38] J. Peukes, T. Betz, Direct measurement of the cortical tension during the growth of membrane blebs, Biophys. J. 107 (8) (October 2014) 1810–1820.
[39] N. Chenouard, I. Smal, F. de Chaumont, M. Maška, I.F. Sbalzarini, Y. Gong, J. Cardinale, C. Carthel, S. Coraluppi, M. Winter, A.R. Cohen, W.J. Godinez, K. Rohr, Y. Kalaidzidis, L. Liang, J. Duncan, H. Shen, Y. Xu, K.E.G. Magnusson, J. Jaldén, H.M. Blau, P. Paul-Gilloteaux, P. Roudot, C. Kervrann, F. Waharte, J.-Y. Tinevez, S.L. Shorte, J. Willemse, K. Celler, G.P. van Wezel, H.-W. Dan, Y.-S. Tsai, C. Ortiz de Solórzano, J.-C. Olivo-Marin, E. Meijering, Objective comparison of particle tracking methods, Nat. Methods 11 (3) (March 2014) 281–289.
[40] S.F. Tolic-Norrelykke, E. Schäffer, J. Howard, F.S. Pavone, F. Jülicher, H. Flyvbjerg, Calibration of optical tweezers with positional detection in the back focal plane, Rev. Sci. Instrum. 77 (10) (2006) (103101–103101–11).
[41] J. Mas, A.C. Richardson, S. Nader, S. Reihani, L.B. Oddershede, K. Berg-Sørensen, Quantitative determination of optical trapping strength and viscoelastic moduli inside living cells, Phys. Biol. 10 (4) (August 2013) 046006.
[42] A.R. Bausch, W. Möller, E. Sackmann, Measurement of local viscoelasticity and forces in living cells by magnetic tweezers, Biophys. J. 76 (1 Pt 1) (1999) 573–579.
[43] M. Puig-de Morales-Marinkovic, M. Grabulosa, J. Alcaraz, J. Mullol, G.N. Maksym, J.J. Fredberg, D. Navajas, Measurement of cell microrheology by magnetic twisting cytometry with frequency domain demodulation, J. Appl. Physiol. 91 (3) (September 2001) 1152–1159.
[44] F. Amblard, B. Yurke, A. Pargellis, S. Leibler, A magnetic manipulator for studying local rheology and micromechanical properties of biological systems, Rev. Sci. Instrum. 67 (3) (March 1996) 818–827.
[45] P. Kollmannsberger, B. Fabry, High-force magnetic tweezers with force feedback for biological applications, Rev. Sci. Instrum. 78 (11) (2007) 114301.
[46] I. De Vlaminck, C. Dekker, Recent Advances in Magnetic Tweezers, Annu. Rev. Biophys. 41 (1) (2012) 453–472.
[47] N. Wang, J.P. Butler, D.E. Ingber, Mechanotransduction across the cell surface and through the cytoskeleton, Science 260 (5111) (May 1993) 1124–1127.
[48] S.M. Mijailovich, M. Kojic, M. Zivkovic, B. Fabry, J.J. Fredberg, A finite element model of cell deformation during magnetic bead twisting, J. Appl. Physiol. 93 (4) (October 2002) 1429–1436.
[49] M. Radmacher, R.W. Tillamnn, M. Fritz, H.E. Gaub, From molecules to cells: imaging soft samples with the atomic force microscope, Science 257 (5078) (September 1992) 1900–1905.
[50] M. Radmacher, R.W. Tillmann, H.E. Gaub, Imaging viscoelasticity by force modulation with the atomic force microscope, Biophys. J. 64 (3) (March 1993) 735–742.
[51] M. Radmacher, Studying the mechanics of cellular processes by atomic force microscopy, Methods Cell Biol. 83 (2007) 347–372.
[52] H. Hertz, Über die Berührung Fester Elastischer Körper (on the contact of elastic solids), J. Reine Angew. Math. 92 (1881) 156–171.
[53] I.N. Sneddon, The relation between load and penetration in the axisymmetric boussinesq problem for a punch of arbitrary profile, Int. J. Eng. Sci. 3 (1) (May 1965) 47–57.
[54] R.E. Mahaffy, C.K. Shih, F.C. MacKintosh, J. Kas, Scanning probe-based frequency-dependent microrheology of polymer gels and biological cells, Phys. Rev. Lett. 85 (4) (July 2000) 880–883.

[55] R.E. Mahaffy, S. Park, E. Gerde, J. Kas, C.K. Shih, Quantitative analysis of the viscoelastic properties of thin regions of fibroblasts using atomic force microscopy, Biophysj. 86 (3) (March 2004) 1777–1793.
[56] T.G. Mason, D.A. Weitz, Optical Measurements of Frequency-Dependent Linear Viscoelastic Moduli of Complex Fluids, Phys. Rev. Lett. 74 (7) (February 1995) 1250–1253.
[57] J.C. Crocker, M.T. Valentine, E.R. Weeks, T. Gisler, P.D. Kaplan, A.G. Yodh, D.A. Weitz, Two-point microrheology of inhomogeneous soft materials, Phys. Rev. Lett. 85 (4) (July 2000) 888–891.
[58] T.M. Squires, T.G. Mason, Fluid Mechanics of Microrheology, Annu. Rev. Fluid Mech. 42 (1) (2010) 413–438.
[59] N. Fakhri, A.D. Wessel, C. Willms, M. Pasquali, D.R. Klopfenstein, F.C. MacKintosh, C.F. Schmidt, High-resolution mapping of intracellular fluctuations using carbon nanotubes, Science 344 (6187) (May 2014) 1031–1035.
[60] M.J. Saxton, K. Jacobson, Single-particle tracking: applications to membrane dynamics, Annu. Rev. Biophys. Biomol. Struct. 26 (1997) 373–399.
[61] J.M. Saxton, Single-particle tracking: the distribution of diffusion coefficients, Biophys. J. 72 (4) (1997) 1744–1753.
[62] H. Qian, M.P. Sheetz, E.L. Elson, Single particle tracking. Analysis of diffusion and flow in two-dimensional systems, Biophys. J. 60 (4) (October 1991) 910–921.
[63] S.S. Rogers, T.A. Waigh, X. Zhao, J.R. Lu, Precise particle tracking against a complicated background: polynomial fitting with Gaussian weight, Phys. Biol. 4 (3) (September 2007) 220.
[64] T. Savin, P.S. Doyle, Static and dynamic errors in particle tracking microrheology, Biophys. J. 88 (1) (January 2005) 623–638.
[65] T. Savin, P.S. Doyle, Role of a finite exposure time on measuring an elastic modulus using microrheology, Phys. Rev. E 71 (4) (2005) 041106.
[66] P. Bursac, B. Fabry, X. Trepat, G. Lenormand, J.P. Butler, N. Wang, J.J. Fredberg, Steven S. An, Cytoskeleton dynamics: fluctuations within the network, Biochem. Biophys. Res. Commun. 355 (2) (April 2007) 324–330.
[67] W. Denk, W.W. Webb, Optical measurement of picometer displacements of transparent microscopic objects, Appl. Opt. 29 (16) (1990) 2382–2391.
[68] F. Gittes, C.F. Schmidt, Interference model for back-focal-plane displacement detection in optical tweezers, Opt. Lett. 23 (1) (January 1998) 7–9.
[69] F. Gittes, C.F. Schmidt, Signals and noise in micromechanical measurements, Methods Cell Biol. 55 (1997) 129–156.
[70] A. Pralle, M. Prummer, E.L. Florin, E.H. Stelzer, J.K. Hörber, Three-dimensional high-resolution particle tracking for optical tweezers by forward scattered light, Microsc. Res. Tech. 44 (5) (March 1999) 378–386.
[71] K.C. Vermeulen, J. van Mameren, G.J.M. Stienen, E. J.G. Peterman, G.J.L. Wuite, C.F. Schmidt, Calibrating bead displacements in optical tweezers using acousto-optic deflectors, Rev. Sci. Instrum. 77 (1) (2006) (013704–013704–6).
[72] T. Betz, M. Lenz, J.-F. Joanny, C. Sykes, ATP-dependent mechanics of red blood cells, Proc. Natl. Acad. Sci. U. S. A. 106 (36) (2009) 15320–15325.
[73] M. Speidel, L. Friedrich, A. Rohrbach, Interferometric 3D tracking of several particles in a scanning laser focus, Opt. Express 17 (2) (January 2009) 1003–1015.
[74] M. Koch, A. Rohrbach, Object-adapted optical trapping and shape-tracking of energy-switching helical bacteria, Nat. Photonics 6 (10) (2012) 680–686.
[75] T. Luo, K. Mohan, P.A. Iglesias, D.N. Robinson, Molecular mechanisms of cellular mechanosensing, Nat. Mater. 12 (11) (November 2013) 1064–1071.
[76] B.D. Hoffman, J.C. Crocker, Cell mechanics: dissecting the physical responses of cells to force, Annu. Rev. Biomed. Eng. 11 (2009) 259–288.
[77] J. Etienne, J. Fouchard, D. Mitrossilis, N. Bufi, P. Durand-Smet, A. Asnacios, Cells as liquid motors: Mechanosensitivity emerges from collective dynamics of actomyosin cortex, Proc. Natl. Acad. Sci. 112 (9) (March 2015) 2740–2745.
[78] S. Ramaswamy, The Mechanics and Statistics of Active Matter, Annu. Rev. Condens. Matter Phys. 1 (9) (April 2010) 1–23.
[79] A. Okubo, Dynamical aspects of animal grouping: swarms, schools, flocks, and herds, Adv. Biophys. 22 (1986) 1–94.
[80] G. de Magistris, D. Marenduzzo, An introduction to the physics of active matter, Physica A: Statistical Mechanics and its Applications 418 (2015) 65–77.
[81] S.C. Takatori, W. Yan, J.F. Brady, Swim Pressure: Stress Generation in Active Matter, Phys. Rev. Lett. (2014).
[82] A. Cavagna, L. Del Castello, I. Giardina, T. Grigera, A. Jelic', S. Melillo, T. Mora, L. Parisi, E. Silvestri, M. Viale, Flocking and turning: a new model for self-organized collective motion, J. Stat. Phys. 158 (3) (2014) 601–627.
[83] A. Attanasi, A. Cavagna, L. Del Castello, I. Giardina, Information transfer and behavioural inertia in starling flocks, Nat. Phys. 10 (9) (2014) 691–696.
[84] N. Kumar, H. Soni, S. Ramaswamy, A.K. Sood, Flocking at a distance in active granular matter, Nat. Commun. 5 (4688) (2014).
[85] W. Bialek, A. Cavagna, I. Giardina, T. Mora, E. Silvestri, M. Viale, A.M. Walczak, Statistical mechanics for natural flocks of birds, Proc. Natl. Acad. Sci. 109 (13) (March 2012) 4786–4791.
[86] D.S. Lemons, A. Gythiel, Paul Langevin's 1908 paper ``On the Theory of Brownian Motion''[``Sur la théorie du mouvement brownien,'' CR Acad. Sci.(Paris)[bold 146], 530–533 (1908)], Am. J. Phys. 65 (1079) (1997).
[87] A. Einstein, On the theory of the Brownian movement, Ann. Phys. 4 (19) (1906) 371–378.
[88] T.G. Mason, Estimating the viscoelastic moduli of complex fluids using the generalized Stokes–Einstein equation, Rheol. Acta 39 (4) (2000) 371–378.
[89] F. Gittes, B. Schnurr, P.D. Olmsted, F.C. MacKintosh, C.F. Schmidt, Microscopic viscoelasticity: shear moduli of soft materials determined from thermal fluctuations, Phys. Rev. Lett. 79 (17) (1997) 3286.
[90] F.C. MacKintosh, J. Kas, P.A. Janmey, Elasticity of semiflexible biopolymer networks, Phys. Rev. Lett. 75 (24) (December 1995) 4425–4428.
[91] D.C. Morse, Viscoelasticity of concentrated isotropic solutions of semiflexible polymers. 1. Model and stress tensor, Macromolecules 31 (20) (1998) 7030–7043.
[92] D.C. Morse, Viscoelasticity of concentrated isotropic solutions of semiflexible polymers. 2. Linear response, Macromolecules 31 (20) (1998) 7044–7067.
[93] É. Fodor, M. Guo, N. Gov, P. Visco, D. Weitz, F. van Wijland, Activity Driven Fluctuations in Living Cells, May 2015 (arXiv:1505.06489).
[94] É. Fodor, K. Kanazawa, H. Hayakawa, P. Visco, F. van Wijland, Energetics of active fluctuations in living cells, Phys. Rev. E 90 (4) (October 2014) 042724.
[95] T. Harada, S.-i. Sasa, Equality connecting energy dissipation with a violation of the fluctuation-response relation, Phys. Rev. Lett. 95 (13) (September 2005) 130602.
[96] O. Chaudhuri, S.H. Parekh, D.A. Fletcher, Reversible stress softening of actin networks, Nature 445 (7125) (January 2007) 295–298.
[97] H. Lee, J. Ferrer, M. Lang, R. Kamm, Molecular origin of strain softening in cross-linked F-actin networks, Phys. Rev. E (2010).
[98] T. Kim, M.L. Gardel, Ed. Munro, Determinants of fluidlike behavior and effective viscosity in cross-linked actin networks, Biophys. J. 106 (3) (February 2014) 526–534.
[99] C. Storm, J.J. Pastore, F.C. MacKintosh, T.C. Lubensky, P.A. Janmey, Nonlinear elasticity in biological gels, Nature 435 (7039) (May 2005) 191–194.
[100] H. Kang, Qi Wen, P.A. Janmey, J.X. Tang, E. Conti, F.C. Mackintosh, Nonlinear elasticity of stiff filament networks: strain stiffening, negative normal stress, and filament alignment in fibrin gels, J. Phys. Chem. B 113 (12) (March 2009) 3799–3805.
[101] T. Kim, W. Hwang, R.D. Kamm, Dynamic role of cross-linking proteins in actin rheology, Biophys. J. 101 (7) (October 2011) 1597–1603.
[102] Y. Yang, M. Bai, W.S. Klug, A.J. Levine, M.T. Valentine, Microrheology of highly crosslinked microtubule networks is dominated by force-induced crosslinker unbinding, Soft Matter 9 (2) (January 2013) 383–393.
[103] K.M. Schmoller, P. Fernandez, R.C. Arevalo, D.L. Blair, A.R. Bausch, Cyclic hardening in bundled actin networks, Nat. Commun. 1 (134) (2010).
[104] T. Liverpool, A. Maggs, A. Ajdari, Viscoelasticity of Solutions of Motile Polymers, Phys. Rev. Lett. 86 (18) (April 2001) 4171–4174.
[105] M. Keller, R. Tharmann, M.A. Dichtl, A.R. Bausch, E. Sackmann, Slow filament dynamics and viscoelasticity in entangled and active actin networks, Philos. Trans. R. Soc. A Math. Phys. Eng. Sci. 361 (1805) (April 2003) 699–711 (discussion 711–2).
[106] D. Smith, F. Ziebert, D. Humphrey, C. Duggan, M. Steinbeck, W. Zimmermann, J. Kas, Molecular motor-induced instabilities and cross linkers determine biopolymer organization, Biophys. J. 93 (12) (December 2007) 4445–4452.
[107] S.K. Vogel, Z. Petrasek, F. Heinemann, P. Schwille, Myosin motors fragment and compact membrane-bound actin filaments, eLife Sci. 2 (2013).
[108] L. Haviv, D. Gillo, F. Backouche, A. Bernheim-Groswasser, A cytoskeletal demolition worker: myosin II acts as an actin depolymerization agent, J. Mol. Biol. 375 (2) (January 2008) 325–330.
[109] T.S. Matsui, R. Kaunas, M. Kanzaki, M. Sato, S. Deguchi, Non-muscle myosin II induces disassembly of actin stress fibres independently of myosin light chain dephosphorylation, Interface Focus 1 (5) (October 2011) 754–766.
[110] X. Trepat, L. Deng, S.S. An, D. Navajas, D.J. Tschumperlin, W.T. Gerthoffer, J.P. Butler, J.J. Fredberg, Universal physical responses to stretch in the living cell, Nature 447 (7144) (May 2007) 592–595.
[111] R. Krishnan, C. Young Park, Y.-C. Lin, J. Mead, R.T. Jaspers, X. Trepat, G. Lenormand, D. Tambe, A.V. Smolensky, A.H. Knoll, J.P. Butler, J.J. Fredberg, Reinforcement versus fluidization in cytoskeletal mechanoresponsiveness, PLoS ONE 4 (5) (2009) e5486.
[112] W.W. Ahmed, T.A. Saif, Active transport of vesicles in neurons is modulated by mechanical tension, Sci. Rep. 4 (4481) (March 2014).
[113] B.R. Parry, I.V. Surovtsev, M.T. Cabeen, C.S. O'Hern, E.R. Dufresne, C. Jacobs-Wagner, The Bacterial Cytoplasm Has Glass-like Properties and Is Fluidized by Metabolic Activity, Cell Camb. MA 156 (1-2) (January 2014) 183–194.
[114] C.J. Chan, A.E. Ekpenyong, S. Golfier, W. Li, K.J. Chalut, O. Otto, J. Elgeti, J. Guck, F. Lautenschläger, Myosin II Activity Softens Cells in Suspension, Biophysj. 108 (8) (April 2015) 1856–1869.
[115] F.C. MacKintosh, A.J. Levine, Nonequilibrium mechanics and dynamics of motor-activated gels, Phys. Rev. Lett. 100 (1) (2008) 18104.
[116] C.P. Broedersz, F.C. MacKintosh, Molecular motors stiffen non-affine semiflexible polymer networks, Soft Matter 7 (7) (2011) 3186.
[118] O.J.N. Bertrand, D. Kuchnir Fygenson, O.A. Saleh, Active, motor-driven mechanics in a DNA gel, Proc. Natl. Acad. Sci. 109 (43) (October 2012) 17342–17347.
[119] W.A. Lam, O. Chaudhuri, A. Crow, K.D. Webster, T.-D. Li, A. Kita, J. Huang, D.A. Fletcher, Mechanics and contraction dynamics of single platelets and implications for clot stiffening, Nat. Mater. 10 (1) (December 2010) 61–66.
[120] A. Chaigne, C. Campillo, N.S. Gov, R. Voituriez, J. Azoury, C. Umaña-Diaz, M. Almonacid, I. Queguiner, P. Nassoy, C. Sykes, M.-H. Verlhac, M.-E. Terret, A soft cortex is essential for asymmetric spindle positioning in mouse oocytes, Nat. Cell Biol. 15 (8) (August 2013) 958–966.
[121] V. Schaller, K.M. Schmoller, E. Karaköse, B. Hammerich, M. Maier, A.R. Bausch, Crosslinking proteins modulate the self-organization of driven systems, Soft Matter 9 (30) (2013) 7229.
[122] V. Schaller, C. Weber, C. Semmrich, E. Frey, A.R. Bausch, Polar patterns of driven filaments, Nature 467 (7311) (September 2010) 73–77.
[123] V. Schaller, C. Weber, E. Frey, A.R. Bausch, Polar pattern formation: hydrodynamic coupling of driven filaments, Soft Matter 7 (7) (2011) 3213–3218.
[124] V. Schaller, C.A. Weber, B. Hammerich, E. Frey, A.R. Bausch, Frozen steady states in active systems, Proc. Natl. Acad. Sci. U. S. A. 108 (48) (2011) 19183–19188.
[125] V. Schaller, A.R. Bausch, Topological defects and density fluctuations in collectively moving systems, Proc. Natl. Acad. Sci. U. S. A. (2013).

[126] S. Köhler, V. Schaller, A.R. Bausch, Structure formation in active networks, Nat. Mater. 10 (6) (June 2011) 462–468.
[127] T. Sanchez, D. Welch, D. Nicastro, Z. Dogic, Cilia-like beating of active microtubule bundles, Science 333 (6041) (July 2011) 456–459.
[128] T. Sanchez, D.T.N. Chen, S.J. DeCamp, M. Heymann, Z. Dogic, Spontaneous motion in hierarchically assembled active matter, Nature 491 (7424) (November 2012) 431–434.
[129] F.C. Keber, E. Loiseau, T. Sanchez, S.J. DeCamp, L. Giomi, M.J. Bowick, M. Cristina Marchetti, Z. Dogic, A.R. Bausch, Topology and dynamics of active nematic vesicles, Science 345 (6201) (September 2014) 1135–1139.
[130] M. Almonacid, W.W. Ahmed, W.W. Bussonnier, M. Mailly, T. Betz, R. Voituriez, M.H. Verlhac, Active diffusion positions the nucleus in mouse oocytes, Nature cell biology (2015).
[131] A.W. Lau, B.D. Hoffman, A. Davies, J.C. Crocker, T.C. Lubensky, Microrheology, stress fluctuations, and active behavior of living cells, Phys. Rev. Lett. 91 (19) (2003) 198101.
[132] C. Wilhelm, Out-of-equilibrium microrheology inside living cells, Physical review letters 101.2 (2008) 028101.
[133] B.D. Hoffman, G. Massiera, K.M. Van Citters, J.C. Crocker, The consensus mechanics of cultured mammalian cells, Proc. Natl. Acad. Sci. U.S.A. 103 (27) (2006) 10259–10264.
[134] P. Martin, A.J. Hudspeth, F. Jülicher, Comparison of a hair bundle's spontaneous oscillations with its response to mechanical stimulation reveals the underlying active process, Proc. Natl. Acad. Sci. 98 (25) (2001) 14380–14385.